AMERICAN HEALTH CONSULTANTS®

CANCER RESEARCH ALERT™

A monthly update of developments in preclinical oncology research for the clinician and researcher

American Health Consultants Home Page—http://www.ahcpub.com

CME for Physicians—http://www.cmeweb.com

XAGE-1, a Cancer Testis Antigen: Potential Use as a Molecular Target for Ewing's Sarcoma

By Kristi A. Egland, PhD, and Tapan K. Bera, PhD

The identification of cancer antigens provides new opportunities for the development of therapeutic strategies against cancer. During the last several years, researchers have developed two major approaches to identify human tumor antigens that are recognized by cytotoxic T lymphocytes (CTL). The first approach is based on direct biochemical purification of tumor antigen peptides from the peptide-MHC complexes, which are recognized by the CTL.[1] The second is a traditional genetic approach to identify tumor antigens; it relies on the generation of a genomic or cDNA library from the tumor cell line. The DNA library is transfected into cells expressing the appropriate MHC molecule. Cells that present peptides derived from proteins encoded by the cDNA library are isolated on the basis of the ability to stimulate cytokine release from CTL.[2] Melanoma antigen (MAGE-1) was the first tumor antigen identified from a human melanoma using the traditional genetic approach.[2]

Subsequently, several cancer antigens have been identified using other approaches, and some of these antigens have been recognized as candidates for cancer vaccines.[3] MAGE-1 is a member of the family of cancer testis (CT) antigens, which is the best characterized group of antigens so far. CT antigens are a distinct class of antigens that are expressed in many types of cancers, yet they have a restricted expression pattern in normal tissues.[4-6]

These genes primarily are expressed in the primitive germ cells, spermotogonia, and normal testis.[7] Some extensively studied CT antigens are MAGE, GAGE, BAGE, and GnT-V and their family members. Although the previously mentioned CT antigens were identified from cDNA libraries derived from a single melanoma tumor cell line, malignant transformation often is associated with activation or depression of silent CT antigens in a wide range of human tumors.[3]

INSIDE

Volume 3 • Number 1 • June 2001 • Pages 1-12

EST Database Mining and Identification of Novel Cancer Antigens

Our laboratory is using a functional genomics approach to discover new genes that are associated with cancer.[8] The cancer genome anatomy project of the National Cancer Institute uses laser-captured microdissection techniques to generate EST libraries. ESTs are partial sequences of cDNA clones randomly selected from various cDNA libraries. Because each of these clones is generated from a single transcript, the number of ESTs for a particular gene from the same library provides valuable information on the expression patterns of genes in different tissues. These EST sequences can be clustered and sorted to identify genes that are preferentially or exclusively expressed in malignant tissues. We have reported a computer screening strategy to identify genes that are preferentially expressed in prostate tumors. By using this screen, we have identified several novel genes, including *PAGE-4*, which is homologous to the GAGE family of cancer testis antigens.[8,9] To discover additional new tumor antigens, we used a "homology walking" program and identified three novel PAGE-GAGE-related genes, including *XAGE-1*. *(See Figure 1.)*

Figure 1

Relatedness of the amino acid sequences of XAGE, PAGE, and GAGE proteins

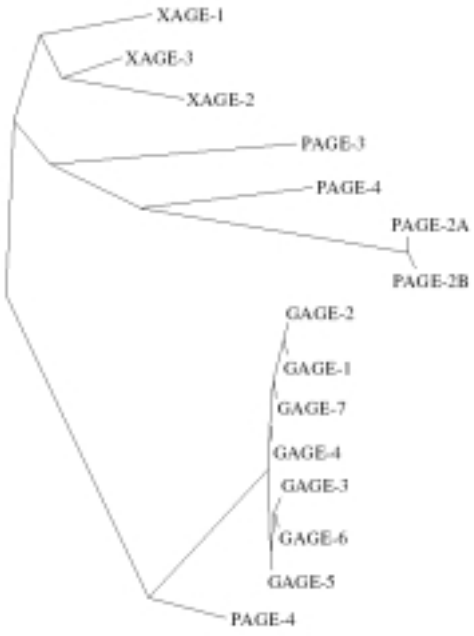

The rooted phylogenetic tree was constructed using the AllAll program from the Computational Biochemistry Research Group (accessed at cbrg.inf.ethz.ch./section3_1.html).

XAGE Expression in Different Tissues

The computer-based screening strategy developed by our group lead to the identification of the novel gene *XAGE-1*.[9] The *XAGE-1* cluster contains ESTs from testis, alveolar rhabdomyosarcoma, Ewing's sarcoma, and germ cell tumor cDNA libraries. *(See Figure 2.)* The *XAGE-1* expression pattern in normal tissues was experimentally determined.[10] A RNA dot blot analysis revealed that *XAGE-1* is expressed in normal testis. A reverse transcriptase-polymerase chain reaction (RT-PCR) analysis, using a human rapid-scan panel containing cDNAs from 24 different tissues of the body, confirmed the high expression of XAGE-1 in normal testis, but also showed that *XAGE-1* was expressed at low levels in lung and peripheral blood lymphocytes (PBL).

However, Northern blot analysis, using a fragment of *XAGE-1* as a probe, revealed a single transcript of approximately 700 bp in testis; no signal was detected in lung or PBL. *(See Figure 3.)* Because Northern blot analysis is less sensitive than RT-PCR, the above results all consistently showed that *XAGE-1* is abundantly expressed in the normal testis only, and weakly expressed in lung and PBL. Based on sequence similarity and expression pattern, *XAGE-1* is a member of the family of CT antigens. The *XAGE-1* gene is located on

Cancer Research Alert, ISSN 1525-3333, is published monthly by American Health Consultants, 3525 Piedmont Rd., NE, Bldg. 6, Suite 400, Atlanta, GA 30305.

Vice President/Group Publisher: Brenda Mooney.
Editorial Group Head: Valerie Loner.
Managing Editor: Suzanne Zunic.
Marketing Manager: Schandale Kornegay.

GST Registration Number: R128870672.

Periodical postage paid at Atlanta GA 30304.
POSTMASTER: Send address changes to ***Cancer Research Alert,*** P.O. Box 740059, Atlanta, GA 30374.

Back issues: $48. One to nine additional copies, $230 each; 10 to 20 additional copies, $172 each.

AMERICAN HEALTH CONSULTANTS™
THOMSON HEALTHCARE

Subscriber Information

Customer Service: 1-800-688-2421

Customer Service E-Mail Address: customerservice@ahcpub.com
Editorial E-Mail Address: suzanne.zunic@ahcpub.com
World-Wide Web: http://www.ahcpub.com

Subscription Prices

United States: $287 per year (Resident rate: $129.50)
Canada: $289 per year plus GST (Resident rate: $144.50)
Elsewhere: $289 per year (Resident rate: $144.50)

Accreditation

American Health Consultants (AHC) is accredited by the Accreditation Council for Continuing Medical Education (ACCME) to provide continuing medical education for physicians.

American Health Consultants designates this continuing medical education activity for up to 30 credit hours in Category 1 credit toward the AMA Physician's Recognition Award. Each physician should claim only those hours of credit that he/she actually spent in the educational activity. This CME activity was planned and produced in accordance with the ACCME Essentials.

For CME credit, add $50.

For Editorial Questions & Comments,

Please call **Suzanne Zunic,** Managing Editor, at (404) 262-5444 between 8:30 a.m. and 4:30 p.m. ET, Monday-Friday.

Statement of Financial Disclosure

In order to reveal any potential bias in this publication, and in accordance with Accreditation Council for Continuing Medical Education guidelines,we disclose that Drs. Egland and Bera, Mr. Handzlik, Dr. Carethers, Ms. Castelli, and Mr. Kessel report no report no financial relationships having ties to this field of study. Dr. Corral, editor-in-chief and author, reports no consultant, stockholder, speaker's bureau, research, or other financial relationships having ties to this field of study.

Figure 2

Composite cluster of EST sequences for *XAGE-1*

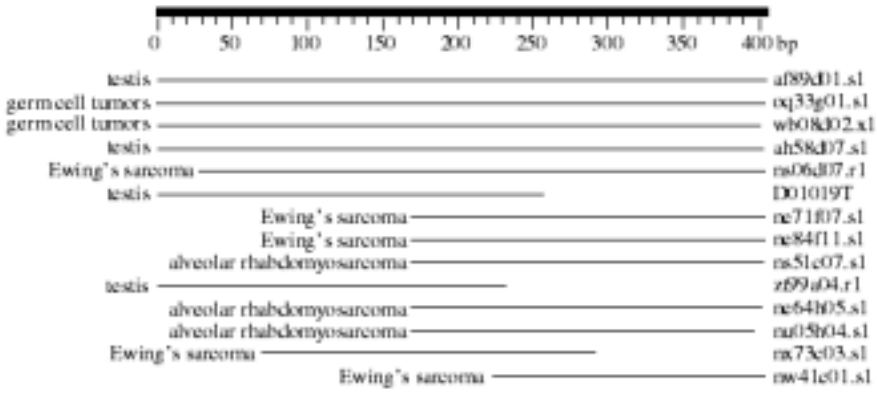

The compiled EST cluster is approximately 410 bp in length and contains 14 ESTs from testis, alveolar rhabdomyosarcoma, Ewing's sarcoma, and germ cell tumor cDNA libraries as indicated. Horizontal lines represent the range of the EST sequences. The EST names are shown on the right.

the X chromosome,[10] which is consistent with the location of other CT antigen genes.[12]

XAGE Expression in Ewing's Sarcoma and Other Cancers

The Ewing's family of tumors include: Ewing's tumor of bone; extraosseus Ewing's (tumor growing outside of the bone); primitive neuroectodermal tumor (PNET), also known as peripheral neuroepithelioma; and Askin's tumor (PNET of the chest wall). These tumors are rare diseases in which cancer cells are found in the bone and soft tissues.[13] This family of tumors has specific chromosomal translocations that result in the fusion of the *EWS* and *FLI1* genes. The FLI1 gene encodes a member of the ETS family of transcription factors,[14] while the widely expressed *EWS* gene encodes a protein of unknown function. The site disrupted by the chromosomal translocation found in the Ewing's sarcoma group of tumors is located in the *EWS* gene.[15] Chromosomal analysis of Ewing's sarcoma has demonstrated that about in 90-95% of cases a t(11;22)(q24;q12) translocation generates an EWS-FLI1 fusion protein, and the precise exon composition of the fusion transcript has been found to be a prognostic marker in this group of tumors.[14] Although the EWS-FLI1 chimeric protein may have therapeutic potential as a molecular target, other tumor-specific targets for Ewing's sarcoma need to be identified.

Our EST database analysis predicts that *XAGE-1* is expressed in alveolar rhabdomyosarcoma and Ewing's sarcom.[9] Consistent with this prediction, *XAGE-1* was expressed in one of one patient samples with alveolar rhabdomyosarcoma and one of three patient samples with embryonal rhabdomyosarcoma. In addition, the *XAGE-1* transcript was present in two of five osteosarcoma cell lines.[10] We also investigated the expression of *XAGE-1* in Ewing's sarcoma. Northern blot analysis revealed an *XAGE-1* transcript in seven of eight Ewing's sarcoma cell lines. *(See Figure 4A.)* Interestingly, the one cell line that does not express XAGE-1 also lacks the EWS-FLI-1 chromosomal translocation. *XAGE-1* also was expressed in four of nine human patient Ewing's sarcoma samples. *(See Figure 4B.)* We found a correlation between the presence of the EWS-FLI-1 or EWS-Erg chromosome translocation and the presence of the *XAGE-1* transcript. However, *XAGE-1* was not expressed in every patient sample that contains the chromosome translocation. The significance of this correlation, and the possibility

Figure 3

Northern blot analysis of *XAGE-1* expression in normal tissues

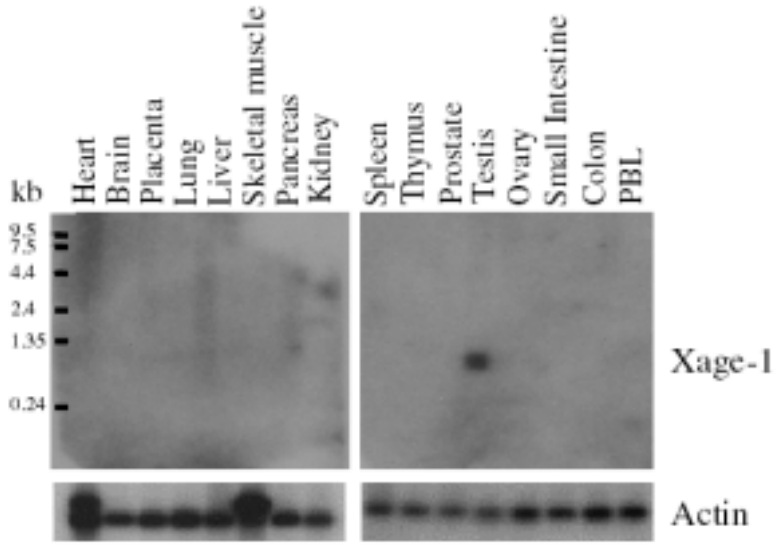

Northern blots containing polyA RNA generated from 16 different normal tissues as indicated were probed with an XAGE-1 fragment followed by an actin probe. The RNA ladder is shown on the left. PBL stands for peripheral blood lymphocytes. The XAGE-1 transcript is approximately 700 bp and is only observed in the testis.

that *XAGE-1* expression could be under the control of the EWS-FLI-1 fusion protein, still remains to be determined.

Figures 4A and B

Northern blot analysis of *XAGE-1* expression in Ewing's sarcoma

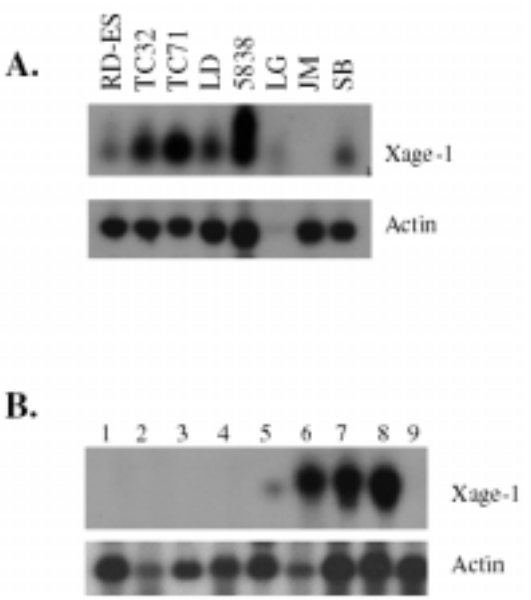

Northern blots containing total RNA from eight Ewing's sarcoma cell lines (A) and nine Ewing's sarcoma patient tumor samples (B) were probed with a fragment of *XAGE-1* and an actin probe separately.

Implications

The ideal cellular target for immunotherapeutic treatment of cancer, such as cancer vaccines or immunotoxins, is one that predominantly has restricted expression in diseased tissues, with some expression in dispensable organs. By using such targets, engineered immunotherapies can kill the tumor cells while sparing the normal tissues. As of yet, good molecular targets for the Ewing's family of tumors still need to be identified. Because *XAGE-1* is expressed in testis and in a large number of Ewing's sarcomas, as well as other cancers, it has good potential for use as a target for various kinds of immunotherapies. *(Dr. Egland is Postdoctoral Fellow and Dr. Bera is Staff Scientist in the Laboratory of Molecular Biology, National Cancer Institute, National Institutes of Health, Bethesda, MD.)* ❖

Acknowledgements

We would like to thank the members of the Gene Discovery Group for their contributions to this project and Ira Pastan for his support and valuable suggestions.

References

1. Mandelboim O, Berke G, Fridkin M, et al. CTL induction by a tumor-associated antigen octapeptide derived from a murine lung-carcinoma. *Nature* 1994;369:67-71.
2. Van der Bruggen P, Traversari C, Chomez P, et al. A gene encoding an antigen recognized by cytolytic T-lymphocytes on a human-melanoma. *Science* 1991;254:1643-1647.
3. Wang RF, Rosenberg SA. Human tumor antigens recognized by T lymphocytes: Implications for cancer therapy. *J Leuk Biol* 1996;60:296-309.
4. De Smet C, Lurquin C, Plaen ED, et al. Genes coding for melanoma antigens recognized by cytolytic lymphocytes. *Eye* 1997;11:243-248.
5. Chen YT, Old LJ. Cancer-testis antigens: Targets for cancer immunotherapy. *Cancer J Sci Am* 1999;5:16-17.
6. Gillespie AM, Rodgers S, Wilson AP, et al. MAGE, BAGE and GAGE: Tumor antigen expression in benign and malignant ovarian tissue. *Br J Cancer* 1998;78: 816-821.
7. Takahashi K, Shichijo S, Noguchi M, et al. Identification of MAGE-1 and MAGE-4 proteins in spermatogonia and primary spermatocytes of testis. *Cancer Res* 1995;55:3478-3482.
8. Vasmatzis G, Essand M, Brinkmann U, et al. Discovery of three genes specifically expressed in human prostate by expressed sequence tag database analysis. *Proc Natl Acad Sci U S A* 1998;95:300-304.
9. Brinkmann U, Vasmatzis G, Lee B, et al. Novel genes in the PAGE and GAGE family of tumor antigens found by homology walking in the dbEST. *Cancer Res* 1999;59:1445-1448.
10. Liu XF, Helman LJ, Yeung C, et al. *XAGE-1,* A new gene that is frequently expressed in Ewing's sarcoma. *Cancer Res* 2000;60:4752-4755.
11. De Plaen E, Arden K, Traversari C, et al. Structure, chromosomal localization, and expression of 12 genes of the *MAGE* family. *Immunogenetics* 1994;40: 360-369.
12. Rogner UC, Wilke K, Steck E, et al. The melanoma antigen gene (MAGE) family is clustered in the chromosomal band Xq28. *Genomics* 1995;29:725-731.
13. de Alava E, Gerald WL. Molecular biology of the Ewing's sarcoma/primitive neuroectodermal tumor family. *J Clin Oncol* 2000;18:204-213.
14. Delattre O, Zucman J, Plougastel B, et al. Gene fusion with an ETS DNA-binding domain caused by chromosome-translocation in human tumors. *Nature* 1992; 359:162-165.
15. Ohno T, Ouchida M, Lee L, et al. The *EWS* gene, involved in Ewing family of tumors, malignant-melanoma of soft parts and desmoplastic small round-cell tumors, codes for an RNA-binding protein with novel regulatory domains. *Oncogene* 1994;9: 3087-3097.

Magnetic Resonance Spectroscopy Imaging, a Diagnostic Tool in Prostate Cancer

By Ryan C. Handzlik, MS, and David A. Corral, MD

The human prostate remains one of the most frequently diseased organs.[1] Prostate cancer has been identified as the most common malignancy in males. Treating prostate cancer at an early stage may be the most effective means of achieving long-term survival, and a number of diagnostic methods have been used to detect and monitor early-stage malignancies. The previously available noninvasive techniques that have been used to diagnose this disease do not adequately differentiate prostate cancer from benign prostatic hyperplasia (BPH) and normal prostatic tissues.[2] The only definitive measure for distinguishing cancer of the prostate from BPH and normal tissue remains a histological analysis of biopsy samples.

Magnetic resonance spectroscopic imaging (MRSI) has been proposed as a noninvasive, diagnostic approach for defining the presence and spatial extent of prostate cancer.[3] The technique potentially can differentiate prostatic adenocarcinoma from BPH and normal prostatic zonal anatomy based on observable metabolite levels present in the prostate. MSRI can be used to measure the distribution of choline and citrate throughout the normal and diseased prostate in an effort to define the presence, extent, and orientation of prostate cancer.[2]

Background

The ability to differentiate areas of prostate cancer from BPH and normal prostatic tissue via a noninvasive approach is important in terms of every aspect of patient care, early cancer staging, and follow-up. Studies using animal models and tissue extracts have identified low levels of citrate and high levels of choline in regions of prostate cancer.[2] Levels of citrate and choline in regions of normal peripheral zone and BPH were used as a baseline for tracking metabolite levels. The differences in metabolite levels in cancer, BPH, and the normal peripheral zone are the focus of the investigations, as 68% of all prostatic cancers occur in the peripheral zone.

The combined use of both localized MRSI and high-resolution MRI of the in situ human prostate has demonstrated lower mean levels of citrate within regions that have been identified as cancerous. It has been proposed that malignant epithelial cells have a diminished capacity for synthesizing and secreting citrate and developing glandular ducts for citrate storage.[2]

Prior to the study by Kurhanewicz and colleagues, changes in choline levels in prostatic cancers were never measured. Choline remains an important metabolite because choline compounds have been implicated in cell membrane synthesis and degradation.[4] Elevations of choline peaks in MR spectra have been reported in a number of human cancers to date. However, the range of metabolite levels associated with normal prostate anatomy, BPH, and cancers of varying grades have not been studied. MRSI has the advantage of providing MR spectra from more than one region, as well as stipulating the exact size and spatial position of the area under investigation. The technique, along with MRI, allows the investigator to measure the distribution of choline and citrate throughout the normal and diseased prostate.

Magnetic Resonance Spectroscopic Imaging of the in situ Human Prostate

In an investigation by Kurhanewicz et al, 3D MRSI, in combination with endorectal MRI techniques, was used to determine the spatial extent of prostate cancer by generating metabolite images and comparing metabolite ratios to normal peripheral zone values present in the prostate. The study was composed of nine healthy volunteers younger than age 40 (ages 28-36), five patients with BPH (ages 63-77), and 85 patients with biopsy-positive prostate cancer (ages 55-75). The results were collected by aligning 3D MRSI data with MRI data, then comparing the results with the pathological findings from biopsy tissue samples. The results of the study identified higher levels of choline and lower levels of citrate in regions of cancer when compared to BPH and normal tissues.[2] Upon completion of MRSI in the 85 prostate cancer patients, significantly lower mean levels of citrate ($P = 0.0001$), and higher mean levels of choline ($P = 0.001$) were detected in regions of cancer when compared to the normal peripheral zone in the same patient.[2]

Hahn and coworkers performed a similar study that displayed potential for the possibility of an in vivo analysis of the prostate using MRSI.[5] They ultimately identified six spectral subregions as having diagnostic potential in prostate tissue. However, in the investigation they found it difficult to integrate only choline resonance in its spectral region because peak overlaps were present in this region of the spectrum. Particularly, this spectral region includes, among other metabolites, creatine resonance. Citrate levels between cancer and BPH were found to be statistically significant. Several hypotheses have been proposed for these findings that have identified an increased amount of the enzyme aconitrase in cancer cells, which contributes to the

break down of citrate.[5] In addition, increased levels of the enzyme ATP-citrate lyase in malignant cells is proposed to contribute to citrate breakdown during lipid synthesis.

The classification of BPH vs. cancer in the Hahn et al study provided MRSI diagnoses that are consistent with histopathology results. These results were directly indicative of the high sensitivity of the technique employed in the study.[5] The results ultimately show that MRSI produces high sensitivity and specificity that can reliably be used for distinguishing between benign and malignant prostatic tissue (100% sensitivity, 95.5% specificity).[5]

Approaches to Prostate Cancer Using Magnetic Resonance Spectroscopy Imaging

Zaider and colleagues describe a method that correlates MRSI data to intraoperatively-obtained ultrasound images and incorporates these data into a treatment planning system for brachytherapy.[6] After MRSI data are obtained, regions of high risk for cancer cells were identified based upon elevated peaks in the MR spectrum. These peaks were then mapped on a spatial grid covering the entire prostate tissue. This technique is followed by an integer-programming procedure in which optimal radioactive seed distribution is determined, and tissue is then implanted within the prostate. This technique is potentially effective, as it may spare surrounding healthy tissues from radioactive dose escalations employed during the course of treatment.

Current treatment-planning algorithms have been developed to determine the ideal placement of radioactive seeds in the prostate. However, uncertainties about tumor position force the delivery of a maximum dose of radiation to the entire prostate gland, which may result in unnecessary dose escalations to the urethra. In the end, the side effects following dose escalation can have an overall effect on the patients' quality of life and adversely result in urinary side effects.[6] MRSI mapping of citrate and choline levels within the prostate can identify regions associated with prostate carcinoma. Ultimately, this approach facilitates the localization of tumors to specific regions within the prostate, and radioactive seeds preferentially can be placed in areas identified with tumor, thus minimizing radiation doses to normal regions.

The results of the study by Zaider et al indicate that the incorporation of clinical data from MRSI into a brachytherapy treatment-planning optimization system is feasible.[6] The findings revealed that dose escalation is critical for improved outcome. The treatment-planning model may lead to local control. In essence, the MRSI-guided treatments direct an increased dose of ^{125}I radioactive seeds to individual target areas in the prostate without adversely affecting healthy tissue surrounding the prostate and the urethra.

Conclusion

The MRSI techniques described enable identification of more sites of carcinoma of the prostate than does prostate biopsy. These results indicate that a larger volume of cancer normally is present upon diagnosis than is indicated by biopsy alone. In patients with detectable elevated prostate specific antigen (PSA), MRSI identified, location-for-location, all foci of prostate carcinoma and benign prostatic tissue that were identified on prostate biopsy.[7] Ultimately, MRSI is superior to transrectal ultrasound and MRI for differentiating carcinoma of the prostate from BPH.[7] In the future, the combined use of endorectal magnetic resonance imaging and MRSI will serve as an invaluable diagnostic tool for differentiating normal from carcinomatous prostate. *(Dr. Corral is Editor-in-Chief of* Cancer Research Alert *and is in the Department of Urologic Oncology, Roswell Park Cancer Institute; Mr. Handzlik is a Graduate Student in the Natural Sciences Program at Roswell Park Cancer Institute, Buffalo, NY.)* ❖

References

1. Greenlee RT, Hill-Harmon MB, Murray T, et al. Cancer Statistics, 2001. *Cancer J Clin* 2001;51:15-36.
2. Kurhanewicz J, Vigneron DB, Hricak H, et al. Three-dimensional H-1 MR spectroscopic imaging of the in situ human prostate with high (0.24-0.7-cm^3) spatial resolution. *Radiology* 1996;198:795-805.
3. Kurhanewicz J, Vigneron DB, Hricak H, et al. Prostate cancer: Metabolic response to cryosurgery as detected with 3D H-1 MR spectroscopic imaging. *Radiology* 1996;200:489-496.
4. Hara T, Kosaka N, Kishi H. PET imaging of prostate cancer using carbon-11-choline. *Nucl Oncol* 1998;39: 990-996.
5. Hahn P, Smith I, Leboldus L, et al. The classification of benign and malignant human prostate tissue by multivariate analysis of ^1H magnetic resonance spectra. *Cancer Res* 1997;57:3398-3401.
6. Zaider M, Zelefsky MJ, Lee EK, et al. Treatment planning for prostate implants using magnetic-resonance spectroscopy imaging. *Int J Radiat Oncol Biol Phys* 2000;47:1085-1096.
7. Parivar F, Hricak H, Shinohara K, et al. Detection of locally recurrent prostate cancer after cryosurgery: Evaluation by transrectal ultrasound, magnetic resonance imaging, and three-dimensional proton magnetic resonance spectroscopy. *Urology* 1996;48:594-599.
8. Pickett B, Vigneault E, Kurhanewicz J, et al. Static field intensity modulation to treat a dominant intraprostatic lesion to 90 GY compared to seven field 3-dimensional radiotherapy. *Int J Radiat Oncol Biol Phys* 1999;43:921-929.

Genetics of Hamartomatous Polyposis Syndromes

By John M. Carethers, MD

Hamartomatous polyposis syndromes are a group of clinically distinct but perhaps genetically related disorders in which the predominant finding is multiple hamartomatous polyps in the gastrointestinal tract. All of these syndromes are transmitted in an autosomal dominant fashion; however, sporadic forms with germline mutations of a gene that is absent from the biological parents have been described. Hamartomatous polyps are characterized by mature but disorganized tissues that are indigenous to the site of origin, and that are not dysplastic. In spite of the benign appearance of the histologic characteristics, each hamartomatous syndrome has an elevated risk for cancer formation at specific organ sites that cannot be fully explained by germline mutations in specific genes because of genetic overlap between the syndromes.

Clinical Features of the Hamartomatous Polyposis Syndromes

Bannayan-Riley-Ruvalcaba syndrome (BRRS), also known as Bannayan-Zonana syndrome, Ruvalcaba-Myhre-Smith syndrome, and Riley-Smith syndrome because of its phenotypic variability, is a rare, congenital syndrome with features that include intestinal juvenile polyps, macrocephaly, subcutaneous and visceral lipomas and hemangiomas, cognitive and motor developmental delay, lipid storage myopathy, Hashimoto's thyroiditis, and pigmentary spotting of the penis in males.[1] Although the prevalence of BRRS syndrome is unknown, patients reported with this syndrome represent sporadic as well as familial occurrences with an autosomal dominant pattern of inheritance.[2]

Juvenile polyposis syndrome (JPS) is a congenital syndrome in which 10 or more juvenile polyps occur in the gastrointestinal tract. Unlike solitary sporadic juvenile polyps, familial juvenile polyps almost always recur after removal. Patients present by age 30, with a mean age of presentation of 9.5 years.[3] The classical symptom is rectal bleeding, but because of the large number of polyps, patients can present with protein loss, malnutrition, cachexia, and failure to thrive.

Both BRRS and JPS patients harbor juvenile polyps within their intestines. Cowden's disease, a syndrome in which multiple hamartomas develop on the skin and mucous membranes (its hallmark is facial trichilemmomas), causes polyps that are distinct from juvenile polyps. While polyps in Cowden's disease may demonstrate a broad range of histology, the most common polyp appears to be a protuberance of cytological normal epithelium that is indigenous to the region from which the polyps arose.[4,5] Hyperplastic polyps also are common. There may be cystic dilation of the glands, fibrosis of the lamina propria, and extension of the muscularis mucosae into the lamina propria. The occurrence of these features allows Cowden's disease polyps to often be histologically confused with juvenile polyps.

Peutz-Jeghers syndrome, with its characteristic mucocutaneous pigmentary spots that appear in association with intestinal hamartomatous polyps, causes a polyp that is distinctive. Peutz-Jeghers polyps demonstrate an arborizing pattern of growth, with the muscularis mucosa extending into branching fronds of the polyp.[3] Benign glands within the polyp may be surrounded by smooth muscle and may extend into the submucosa or muscularis propria (pseudoinvasion). Hereditary mixed polyposis syndrome is a recently described syndrome in which affected family members have atypical juvenile polyps, hyperplastic polyps, colonic adenomas, and colonic adenocarcinomas.[6] Although this syndrome can present with atypical juvenile polyps, its gene has been linked to chromosome 6q in one extended family,[7] and not to the chromosomal sites that have been implicated for BRRS, JPS, and Cowden's disease.

Genes Involved with the Hamartomatous Polyposis Syndromes

Germline mutations in three genes are associated with the hamartomatous polyposis syndromes. The first is *SMAD4*, which encodes a key intracellular signal transducer and transcriptional regulator for the TGFβ superfamily of ligands and receptors. In the colon, the effect of TGFβ action is growth suppression. Thus, uncoupling TGFβ action by mutational inactivation of *SMAD4* would have the net effect of cellular proliferation. The second is *PTEN*, which encodes a dual-specific phosphatase (phosphoserine/phosphothreonine and phosphotyrosine residues) that can dephosphorylate proteins (FAK and others), but more importantly lipids (PIP3 and PI3,4P2). PTEN is a tumor suppressor protein which, by its dephosphorylating ability, contributes to programmed cell death and inhibits the cell's ability to migrate and invade. Thus, mutational inaction of PTEN would remove these phenotypes, and have the net effect of cellular proliferation and enhancing cell migration and invasion. The third is *STK11*, which encodes a protein with homology to serine/threonine kinases. The pathway(s) that involve *STK11* have not been elucidated.

A total of 87 germline mutations of *PTEN* have been described for Cowden's disease, BRRS, and JPS at the end of the year 2000.[8] Fewer mutations of *SMAD4*, all of them causing truncation of the protein, have been demonstrated solely in the germline of JPS patients. Mutations in *STK11* exclusively occur in the germline of

Table

Hamartomatous polyposis syndromes and their associated germline-mutated genes

Hamartomatous Syndrome	Chromosomal Location	Mutated Gene	Frequency in Germline
Hereditary Mixed Polyposis Syndrome	6q	unknown	—
Juvenile Polyposis (JPS)	18q21.1 10q22.3-24.1	*SMAD4* *PTEN/MMAC1/TEP1*	21-50% < 10%
Bannayan-Riley-Ruvalcaba (BRRS)	10q23	*PTEN/MMAC1/TEP1*	50%
Cowden's Disease (CD)	10q22-23	*PTEN/MMAC1/TEP1*	> 80%
Peutz-Jeghers Syndrome	19p13.3	*STK11*	> 90%

patients with Peutz-Jeghers syndrome. There is no clear genotype-phenotype correlation in these syndromes.

BRRS, JPS, and Cowden's Disease: One Disease or Multiple Syndromes?

BRRS and JPS might be variants of each other because they share the common feature of intestinal juvenile polyposis, and are both transmitted in an autosomal dominant fashion to offspring. Patients with JPS are predisposed to juvenile hamartomatous polyps and gastrointestinal cancer, with a 15% incidence of colorectal carcinoma in young patients and a cumulative risk of 68% by age 60.[9-12] Since the lifetime risk for sporadic colorectal cancer in the United States is about 5%, patients with JPS have a four- to 12-fold elevated risk of developing colorectal carcinoma. Peutz-Jeghers and Cowden's disease do not carry an increased risk for colorectal cancers, although Peutz-Jeghers syndrome does have a higher incidence of early-onset cancers of the stomach, duodenum, and pancreas, and Cowden's disease patients have a propensity for breast and thyroid cancers.[3]

DNA microsatellite markers were used to genetically map a BRRS patient by deletional analysis with an aberration involving chromosome 10q, between 10q23.2 and 10q24.1.[2] This area matched an area of deletion also described for a JPS patient with multiple congenital abnormalities,[13] and the Cowden critical region linked to chromosome 10q23.[14] Some phenotypic features of BRRS have been described that overlap with those commonly found in Cowden's disease. Facial trichilemmomas have been described in BRRS,[15] and three BRRS kindreds have been described in which some members developed thyroid follicular neoplasms.[15,16] These phenotypic descriptions, along with Cowden's disease and BRRS and some patients with JPS commonly mapping to chromosome 10q23, originally supported the possibility that the same gene may be responsible for all of these described syndromes.

The mapped region on chromosome 10q23 that is common to these syndromes was found to contain the *PTEN* tumor suppressor gene, also known as *MMAC1* and *TEP1*.[17-19] Thereafter, two BRRS families demonstrated germline mutations in *PTEN* (one family demonstrated a missense mutation, and one showed a truncating mutation).[20] Thus, loss of chromosome 10q23 and germline mutations of *PTEN* can cause the phenotype of BRRS. Germline *PTEN* mutations also have been identified in four of five families with Cowden's disease,[21] and in four families with JPS.[22,23] Genetically, germline mutations in *PTEN* make BRRS, Cowden's disease, and JPS allelic with each other, at least in some families. *PTEN* encodes a dual-specificity phosphatase with homology to tensin and auxillin, and has two potential tyrosine phosphate acceptor domains.[17,19] Identical germline mutations in *PTEN* at codon 233, which cause a truncation mutation at one potential tyrosine phosphate acceptor site, have been reported in one family with BRRS and one with Cowden's disease.[20,21] Additionally, a mother with Cowden's disease had a child with BRRS, with expected identical germline mutations in *PTEN*.[24] As mentioned, BRRS, JPS, and Cowden's disease appear clinically distinct. Although BRRS and JPS share juvenile polyps as common features and may be variants of each other, juvenile polyps are not common lesions in Cowden's disease.[4,5] In addition, the risk of colon cancer is elevated four- to 12-fold in JPS but not in Cowden's disease,[10,11] and has not been ascertained in BRRS.

While the majority of Cowden's disease families demonstrate germline mutations in *PTEN*,[25] this has not been the case for JPS and BRRS. Linkage mapping in eight informative JPS families excluded chromosome 10q22-24 as the susceptibility locus for JPS. Furthermore, 14 families with JPS and 11 sporadic JPS cases lacked *PTEN* mutations by denaturing gradient gel electrophoresis and direct DNA sequencing.[26,27] A large Iowa kindred with JPS demonstrated linkage to chromosome 18q21.1.[27] Subsequently, three familial and two sporadic JPS cases out of a total of nine demonstrated germline mutations in the *SMAD4* gene at chromosome 18q21.1,[28] whose gene product is a critical component of TGFβ1 signal transduction. The most common *SMAD4* mutation was a four-bp deletion from codons 414-416; a 2 bp deletion from codon 348 and a 1-bp insertion at codon 229 also were reported. All of these mutations are predicted to cause a truncated SMAD4 protein and prevent homotrimerization at its carboxyl terminus. Moreover, we failed to demonstrate any deletion of chromosome 10q23 and any germline mutation in *PTEN* in three BRRS patients.[29] The frequency of finding *PTEN* germline mutations in BRRS is much lower

than that observed for Cowden's disease.[25] Thus, the reports of BRRS and JPS patients demonstrating germline *PTEN* mutations constitute only a portion of the genetic etiology for these diseases. The discovery of a perturbation in the TGFβ1 signaling pathway in JPS implicates other components of this transduction pathway in causing JPS and BRRS. SMAD2, another component of the TGFβ signaling pathway and one that heterodimerizes with SMAD4, and SMAD4 appear not to be mutated in the three BRRS patients without germline *PTEN* mutations above (our unpublished observations).

Conclusions

The hamartomatous intestinal polyposis syndromes are inherited as autosomal dominant diseases. The genes involved in these syndromes are predicted to act in a recessive manner in the "target" tissue (i.e., they are tumor suppressor genes and require inactivation of both alleles), in accordance with the Knudson hypothesis. Germline mutations reported for the hamartomatous polyposis syndromes are listed in the Table.

Germline mutations in *STK11* appear to cause the phenotype of Peutz-Jeghers syndrome exclusively. Likewise, germline mutations of *SMAD4* appear to only cause the phenotype of JPS. Germline mutation of *PTEN*, however, is associated with the phenotypes seen in Cowden's disease, BRRS, and in some JPS patients. Thus, genetic similarity exists and causes phenotypic heterogeneity (i.e., mutations in *PTEN* are associated with three hamartomatous syndromes), and genetic heterogeneity exists and causes phenotypic similarity (i.e., mutations in *PTEN* and *SMAD4* are associated with JPS). There are likely other factors that affect these genes to modify the phenotype and each syndrome's cancer risk. Additional genes likely are involved in at least BRRS and JPS families, as the described mutations in *PTEN* and *SMAD4* do not account for all of the patients with these syndromes. *(Dr. Carethers is Staff Gastroenterologist, VA San Diego Healthcare System, GI Section, University of California, San Diego.)* ❖

Acknowledgements

This study was supported by a grant from the U.S. Public Health Service (NCI R01 90231).

References

1. Gorlin RJ, Cohen Jr MM, Condon LM, et al. Bannayan-Riley-Ruvalcaba syndrome. *Am J Med Genet* 1992;44:307-314.
2. Zigman AF, Lavine JE, Jones MC, et al. Localization of the Bannayan-Riley-Ruvalcaba syndrome to chromosome 10q23. *Gastroenterol* 1997;113:1433-1437.
3. Burt R. Polyposis syndromes. In: Yamada T, ed. *Textbook of Gastroenterology*, 2nd ed. 1995:1944-1966.
4. Haggitt, RC, Reid BJ. Hereditary gastrointestinal polyposis syndromes. *Am J Surg Pathol* 1986;10:871-887.
5. Marra G, Armelao F, Vecchio FM, et al. Cowden's disease with extensive gastrointestinal polyposis. *J Clin Gastroenterol* 1994;18:42-47.
6. Whitelaw SC, Murday VA, Tomlinson IPM, et al. Clinical and molecular features of the hereditary mixed polyposis syndrome. *Gastroenterol* 1997;112:327-334.
7. Thomas HJW, Whitelaw SC, Cottrell SE, et al. Genetic mapping of the hereditary mixed polyposis syndrome to chromosome 6q. *Am J Hum Genet 1996;*58:770-776.
8. Bonneau D, Longy M. Mutations of the human *PTEN* gene. *Hum Mutat* 2000;16:109-122.
9. Heiss KF, Schaffner D, Ricketts RR, et al. Malignant risk in juvenile polyposis coli: Increasing documentation in the pediatric age group. *J Ped Surg* 1993;28:1188-1193.
10. Jass JR, Williams CB, Bussey HJR, et al. Juvenile polyposis—A precancerous condition. *Histopathol* 1988;13:619-630.
11. Giardiello FM, Hamilton SR, Kern SE, et al. Colorectal neoplasia in juvenile polyposis or juvenile polyps. *Arch Dis Child* 1991;66:971-975.
12. Jarvinen HJ, KO Franssila. Familial juvenile polyposis coli; increased risk of colorectal cancer. *Gut* 1984;25: 792-800.
13. Jacoby RF, Schlack S, Sekhon G, et al. Del (10)(q22.3q24.1) associated with juvenile polyposis. *Am J Med Genet* 1997;70:361-364.
14. Nelen MR, Padberg GW, Peeters EAJ, et al. Localization of the gene for Cowden disease to chromosome 10q22-23. *Nature Genet* 1996;13:114-116.
15. Fargnoli, MC, Orlow SJ, Semel-Concepcion J, et al. Clinicopathologic findings in the Bannayan-Riley-Ruvalcaba syndrome. *Arch Dermatol* 1996;132:1214-1218.
16. Miles JH, Zonana J, Mcfarlane J, et al. Macrocephaly with hamartomas: Bannayan-Zonana syndrome. *Am J Med Genet* 1984;19:225-234.
17. Li J, Yen C, Liaw D, et al. PTEN, a putative protein tyrosine phosphatase gene mutated in human brain, breast and prostate cancer. *Science* 1997;275:1943-1947.
18. Li D-M, Sun H. TEP1, encoded by a candidate tumor suppressor locus, is a novel protein tyrosine phosphatase regulated by transforming growth factor β. *Cancer Res* 1997;57:2124-2129.
19. Steck PA, Pershouse MA, Jasser SA, et al. Identification of a candidate tumour suppressor gene, *MMAC1,* at chromosome 10q23.3 that is mutated in multiple advanced tumors. *Nat Genet* 1997;15:356-362.
20. Marsh DJ, Dahia PLM, Zheng Z, et al. Germline mutations in *PTEN* are present in Bannayan-Zonana syndrome. *Nat Genet* 1997;16:333-334.
21. Liaw D, Marsh DJ, Li J, et al. Germline mutations of the *PTEN* gene in Cowden disease, an inherited breast

and thyroid cancer syndrome. *Nat Genet* 1997;16:64-67.
22. Olschwang S, Serova-Sinilnikova OM, Lenoir GM, et al. *PTEN* germ-line mutations in juvenile polyposis coli. *Nat Genet* 1998;18:12-13.
23. Huang SC, Chen CR, Lavine JE, et al. Genetic heterogeneity in familial juvenile polyposis. *Cancer Res* 2000;60:6882-6885.
24. Zori RT, Marsh DJ, Graham GE, et al. Germline *PTEN* mutation in a family with Cowden syndrome and Bannayan-Riley-Ruvalcaba syndrome. *Am J Med Genet* 1998;80:399-402.
25. Marsh DJ, Coulon V, Lunetta KL, et al. Mutations spectrum and genotype-phenotype analyses in Cowden disease and Bannayan-Zonana syndrome, two hamartoma syndromes with germline *PTEN* mutations. *Hum Mol Genetics* 1998;7:505-517.
26. Marsh DJ, Roth S, Lunetta K, et al. Exclusion of PTEN and 10q22-24 as the susceptibility locus for juvenile polyposis syndrome. *Cancer Res* 1997;57:5017-5021.
27. Howe JR, Ringold JC, Summers RW, et al. A gene for familial juvenile polyposis maps to chromosome 18q21.1. *Am J Hum Genet* 1998;62:1129-113.
28. Howe JR, Roth S, Ringold JC, et al. Mutations in the *SMAD4/DPC4* gene in juvenile polyposis. *Science* 1998;280:1086-1088.
29. Carethers JM, Furnari FB, Zigman AF, et al. Absence of *PTEN/MMAC1* germline mutations in sporadic Bannayan-Riley-Ruvalcaba syndrome. *Cancer Res* 1998;58:2724-2726.

Potentiation of Photodynamic Therapy by Ursodeoxycholic Acid

By Michelle Castelli and David Kessel, PhD

Photodynamic therapy (PDT) is a procedure used to bring about selective photodamage to neoplastic tissues. PDT involves the use of photosensitizing agents that tend to localize somewhat selectively in neoplastic tissues, tumor vasculature, and other sites that are spared from toxicity, since irradiation is needed to "activate" these agents. The determinants of localization are not yet clear. PDT also has been used for treatment of vascular diseases, e.g., atherosclerotic plaque and macular degeneration. A general review of the field was recently published.[1] Several photosensitizing agents have been identified with the sufficient selectivity for pathologic vs. normal tissues to be clinically useful. Irradiation of cells treated with one class of sensitizers results in a rapid loss of the mitochondrial membrane potential ($\Delta\psi_m$). This is accompanied by the translocation of cytochrome c to the cytosol, followed by the prompt initiation of an apoptotic response.[2] The resulting mode of cell death is mediated by the pathway leading to caspase 3 activation initially identified by Wang's group.[3] We reported that an important target for this class of photosensitizing agents is the anti-apoptotic protein bcl-2.[4] A recent report indicated that the efficacy of this group of photosensitizers could be promoted by a bile acid in current clinical use for other indications.[5] Another group of photosensitizing agents targets lysosomes for photodamage.[6] Preliminary studies indicate that the photodynamic properties of these agents are not promoted by bile acids.

Background

The bile acid UDCA (ursodeoxycholic acid) commonly is used for the solubilization of gallstones and in the treatment of biliary cirrhosis.[7] UDCA has been shown to protect hepatocytes, hepatoma, osteogenic sarcoma, and HeLa cells from apoptosis induced by a variety of stimuli, including okadaic acid, hydrogen peroxide, ethanol, and deoxycholic acid.[8] In the latter case, UDCA prevented both loss of $\Delta\psi_m$ and release of cytochrome c from mitochondria into the cytosol.[9,10] These results suggest that UDCA can protect mitochondria from adverse effects that may lead to the opening of the mitochondrial pore and the release of cytochrome c, a trigger for the apoptotic program.

Deoxycholate is a more hydrophobic analog of UDCA. The ability of deoxycholate to elicit an apoptotic response[10] could be a result of the amphipathic properties of this agent, since exposure of cells to detergents such as Triton X-100 also results in apoptotic death.[11] If the release of cytochrome c is mediated by chaotropic interactions with the mitochondrial membrane, the protective effect of UDCA could be derived from competition with more hydrophobic agents for mitochondrial binding sites. Such a competition could not, however, explain the protection from hydrogen peroxide and ethanol.

Based on the ability of UDCA to protect mitochondria from stimuli that lead to an apoptotic response, we considered it highly probable that this agent also would protect cells from apoptosis induced by photodynamic therapy.

Experimental Approach

To evaluate the potential for UDCA-induced changes in PDT phototoxicity, we carried out studies using two different murine neoplastic cell lines, the L1210 lymphoblastic leukemia, and the 1c1c7 hepatoma.[5] In contrast to data previously reported, we found that UDCA enhanced the cytotoxic response to PDT. At levels as low as 20 μM, a substantial increase in PDT efficacy by UDCA was observed when cells were sensitized with

agents that target bcl-2 for photodamage.[6] Treatment with UDCA enhanced caspase-3 activation, appearance of apoptotic morphology, and loss of cell viability after irradiation. UDCA promoted loss of $\Delta\psi_m$ and release of cytochrome c into the cytosol after photodamage. Controls were carried out to demonstrate that UDCA alone, at levels as high as 100 μM, did not result in cytochrome c release into the cytosol or any loss of cell viability.

It is known that the administration of UDCA in man results in a substantial conversion of UDCA to the glycine and taurine conjugates GUDCA and TUDCA, respectively.[12] We considered it important to evaluate these potential detoxification products for activity. Neither GUDCA nor TUDCA was cytostatic or cytotoxic to L1210 cells, but both conjugates were as active as UDCA in potentiating the cytotoxic effects of PDT.[5] Such a result is interpreted to mean that UDCA catabolism will not decrease the effectiveness of the product.

The promotion of PDT efficacy could be explained if UDCA acted to lower the threshold for photodamage to bcl-2. This could occur if an interaction between UDCA and bcl-2 resulted in a conformational change such that certain regions of the protein were better exposed to the photosensitizers. A second possibility is that UDCA alters the mitochondrial pore, resulting in an enhanced interaction with the pro-apoptotic protein bax. It has been established that bax is not affected by PDT under conditions where bcl-2 is sufficiently altered so as not to be detectable on Western blot.[4] It also is possible that the interaction between UDCA and the mitochondrial membrane results in the promotion of sensitizer binding. In this case, direct photodamage to the membrane could result in release of cytochrome c without any intermediate steps.

Conclusions

Photodynamic therapy currently is being investigated as a means for selective tumor eradication.[1] It has been demonstrated that UDCA can promote the phototoxic response to PDT when used in conjunction with photosensitizing agents that initially catalyze alterations in the bcl-2 molecule. A variety of clinically-useful agents fall into this class, including Photofrin, protoporphyrin derived from administration of 5-aminolevulinic acid,[13] m-tetrahydroxyphenyl-chlorin (mTHPC), and the etiopurpurin SnET2.[1] These agents have either received FDA approval for photodynamic therapy or are in clinical trials.

Several other procedures have been suggested for enhancing the efficacy of PDT, including fractionated light dose[14] and hyper-oxygenation of tissues.[15] The use of UDCA may be a simpler approach to this same end. Since UDCA has a long history of clinical safety,[7] addition of this agent to a clinical protocol might present minimal challenge with regard to potential adverse reactions, although the effect on selectivity remains to be established. It is noteworthy that the taurine and glycine conjugates of UDCA also enhance PDT efficacy, since metabolism of UDCA to these conjugates readily occurs in man.[16] Further studies with animal models are underway to determine whether UDCA pharmacokinetics will be suitable for promotion of PDT responses.

Photodynamic therapy is known to cause loss of viability of malignant cells by several mechanisms.[1] These include direct cell kill, vascular shutdown, and the evoking an enhanced immunologic response. Direct cell kill can eradicate, at best, two tumor logs, meaning that seven doublings will restore the initial tumor mass. Vascular shutdown likely provides the additional cell kill that accounts for the tumor eradication commonly seen after PDT. Immunologic phenomena are now being examined as an additional factor in PDT efficacy. At this stage in the investigation, it is apparent that one effect of UDCA is the enhancement of the direct tumor cell kill after PDT. Effects on vascular shutdown and immune effects remain to be explored. *(Dr. Kessel is a Professor of Pharmacology and Medicine, and Ms. Castelli is a graduate student in the Cancer Biology Program, Department of Pharmacology, Wayne State University School of Medicine, Detroit, MI.)* ❖

References

1. Dougherty TJ, Gomer CJ, Henderson BW, et al. Photodynamic therapy. *J Natl Cancer Inst* 1983;90:889-905.
2. Kessel D, Luo Y. Photodynamic therapy: A mitochondrial inducer of apoptosis. *Cell Death Differ* 1999;6:28-35.
3. Budihardjo I, Oliver H, Lutter M, et al. Biochemical pathways of caspase activation during apoptosis. *Annu Rev Cell Dev Biol* 1999;15:269-290.
4. Kim HR, Luo Y, Li G, et al. Enhanced apoptotic response to photodynamic therapy after bcl-2 transfection. *Cancer Res* 1999;59:3429-3432.
5. Kessel D, Caruso JA, Reiners JJ Jr. Potentiation of photodynamic therapy by ursodeoxycholic acid. *Cancer Res* 2000;60:6985-6988.
6. Kessel D, Luo Y, Deng Y, et al. The role of subcellular localization in initiation of apoptosis by photodynamic therapy. *Photochem Photobiol* 1997;65:422-426.
7. Heathcote EJ. Management of primary biliary cirrhosis. *Hepatology* 2000;31:1005-1013.
8. Mitsuyoshi H, Nakashima T, Sumida Y, et al. Ursodeoxycholic acid protects hepatocytes against oxidative injury via induction of antioxidants. *Biochem Biophys Res Commun* 1999;263:537-542.
9. Rodrigues CM, Fan G, Ma X, et al. A novel role for ursodeoxycholic acid in inhibiting apoptosis by modulating mitochondrial membrane perturbation. *J Clin Invest* 1998;101:2790-2799.
10. Botla R, Spivey JR, Aguilar H, et al. Ursodeoxycholate

(UDCA) inhibits the mitochondrial membrane permeability transition induced by glycochenodeoxycholate: A mechanism of UDCA cytoprotection. *J Pharmacol Exp Ther* 1995;272:930-938.
11. Borner MM, Schneider E, Pirnia F, et al. The detergent Triton X-100 induces a death pattern in human carcinoma cell lines that resembles cytotoxic lymphocyte-induced apoptosis. *FEBS Lett* 1994;353:129-132.
12. Crosignani A., Setchell KD, Invernizzi P, et al. Clinical pharmacokinetics of therapeutic bile acids. *Clin Pharmacokinet* 1996;30:333-358.
13. Wilson BC, Olivo M, Singh G. Subcellular localization of photofrin and aminolevulinic acid and photodynamic cross-resistance in vitro in radiation-induced fibrosarcoma cells sensitive or resistant to photofrin-mediated photodynamic therapy. *Photochem Photobiol* 1997;65:166-176.
14. Curnow A, McIlroy BW, Postle-Hacon MJ, et al. Light dose fractionation to enhance photodynamic therapy using 5-aminolevulinic acid in the normal rat colon. *Photochem Photobiol* 1999;69:71-76.
15. Maier A, Anegg U, Tomaselli F, et al. Does hyperbaric oxygen enhance the effect of photodynamic therapy in patients with advanced esophageal carcinoma? A clinical pilot study. *Endoscopy* 2000;32:42-48.

Funding News

Department of Defense Ovarian Research Program

The U.S. Department of Defense will once again continue funding its Ovarian Cancer Research Program in 2001. This program encourages scientific inquiry of ovarian cancer and peritoneal carcinoma focusing on the aspect of etiology, early diagnosis, therapeutics, and quality of life. Two areas that are being emphasized this year include prevention in behavioral studies. Institutions that do not already have an Ovarian Cancer Research Program project award will be given preference. Research project grants are limited to $300,000 per year for three years. Those wishing to apply must submit a letter of intent as soon as possible but definitely prior to July 3, 2001; the deadline for final application is July 18, 2001. Funding will be awarded in three areas: 1) Research project grants; new investigator research award; and idea awards. Further information is available at the website http://mrmc-rad6.army.mil/funding/default.htm#ocrp.

Mesothelioma Applied Research Foundation Mesothelioma Research Grant

The Mesothelioma Applied Research Foundation (MARF) was established after recognition that funding for this disease has been disproportionately low compared to other diseases. The foundation has enlisted basic science and clinical experts in this field to advance research in this area. The MARF offers researchers grants of up to $500,000 over a two-year period for mesothelioma treatment research, contingent upon funds being available. The MARF currently is accepting applications for the funding of both basic science and clinical research grants. The current proposal allows funding of up to $50,000 per year for up to two years. This grant is intended to support mesothelioma treatment research, and investigations into the disease's etiology will not be supported by this particular grant mechanism. The deadline for application is June 15, 2001. Applications will be limited to 10 pages. There is a very rapid turnover time for processing these grant applications, with review to be completed by the MARF by July 31 and awards to be activated by Aug. 31, 2001. More information can be obtained from MARF by calling (805) 560-8942 or by accessing the MARF website at http://www.marf.org\Grants\Grants.htm. ❖

CME Questions

21. Magnetic resonance spectroscopy imaging (MRSI) of prostate cancer has identified high levels of:
a. pyrophosphate.
b. citrate.
c. choline.
d. acetate.

22. Hamartomatous polyposis syndromes are characterized by:
a. multiple polyps in the gastrointestinal tract.
b. autosomal dominant transmission fashion; however, sporadic forms with germline mutations of a gene absent from the biological parents have been described.
c. polyps with mature but disorganized tissue.
d. All of the above

23. The *XAGE-1* gene is located on which of the following chromosomes?
a. 7
b. 8
c. 10
d. X

24. Other than its potential use in photodynamic therapy, ursodeoxycholic acid is commonly used for:
a. the solubilization of kidney stones and in the treatment of renal disease.
b. the solubilization of gallstones and in the treatment of biliary cirrhosis.
c. the treatment of hemolytic anemia.
d. the treatment of HIV infection

In Future Issues: Stress-Induced Genetic Instability